Athermal design of the mirror support with flexure hinges for the laser communication terminal*

YANG Feng-fu (杨丰福)[1,2], **TIAN Hai-ying** (田海英)[1]**, **YAN Chang-xiang** (颜昌翔)[1,3], **WU Cong-jun** (吴从均)[1], **and MU De-qiang** (母德强)[4]

1. *Changchun Institute of Optics, Fine Mechanics and Physics, Chinese Academy of Sciences, Changchun 130033, China*
2. *University of Chinese Academy of Sciences, Beijing 100049, China*
3. *Center of Materials Science and Optoelectrics Engineering, University of Chinese Academy of Science, Beijing 100049, China*
4. *Changchun University of Technology, Changchun 130012, China*

(Received 29 January 2019; Revised 10 April 2019)

In order to suppress the effect of the temperature variation on the wavefront of the laser communication terminal, the secondary mirror support with flexure hinges is designed. The series-wound straight-circle flexure hinge is designed to achieve the maximal variation range of the flexibility or stiffness with the limit of flexure hinges' geometrical size. The position and quantity of the flexure hinges are determined to control the deformation direction of the secondary mirror. In order to search the direction in which the wavefront aberration is minimum, the flexure hinges' parameters are optimized with the system wavefront aberration as the optimization objective. The prototype of the laser communication terminal is constructed and the value of the wavefront aberration is measured under the condition of 20±2°C. Experimental results show that the value of the wavefront aberration root mean square (*RMS*) is reduced from 0.066λ to 0.042λ, meeting the requirement of *RMS* less than 1/20λ (λ=632.8 nm). The athermal design method presented in this paper provides a novel way for the athermal design of the small aperture mirror support in off-axis optical systems.

Document code: A **Article ID:** 1673-1905(2019)06-0454-5
DOI https://doi.org/10.1007/s11801-019-9017-1

With the excellent characteristics of small size, light weight, low power, high data rate, strong anti-interference and anti-intercept, the prospect of laser communication is brilliant[1,2]. As the key component of the laser communication terminal, the mirror support acts as keeping the position of the mirror within the specific tolerance. Deformation of the mirror support brought about by the variation of the temperature will result in the distortion and movement of the mirror, which seriously affects the performance of the terminal[3]. Thus, it is of great importance to conduct athermal design for the mirror support.

At present, the main methods of athermal design are as follows: mechanical passive athermal, electromechanical active athermal and optical passive athermal. Taking into consideration of the reliability, mass and performance, the mechanical passive athermal are widely used. Li Shen-hua et al[4] designed a mirror flexure support with the notch of straight circular for a 1.5 m diameter mirror, Liu Ming et al[5] designed a neck side grooving flexure mirror support for laser communication system, and Ren Guo-rui et al[6] designed an inverted bipod flexible mirror support for a space telescope. The mirror support designed above effectively reduced the deformation influence of mirror support on the mirror and improved the performance of the optical system. However, the researches on the athermal design mainly focus on the effect of the temperature on the mirror surface and the effect of the movement of the mirror has rarely been studied to reduce the performance degradation of the laser communication terminal optical system caused by the variation of the temperature.

In this paper, the layout of the flexure hinges is studied to control the deformation direction of the mirror caused by the temperature variation and the athermal design method of the mirror support is conducted by optimizing the parameters of the flexure hinges based on the integrated optimization model.

Considering the requirement of high obstruction ratio, the design of the off-axis two-mirror system is adopted in the laser communication terminal optical system and consists of two mirrors with off-axis paraboloid which

* This work has been supported by the National High Technology and Development Program of China (No.2016YFF0103603), and the National Natural Science Foundation of China (No.6187030909).
** E-mail: tianhy@ciomp.ac.cn

possess the superior focusing performance for parallel rays, as shown in Fig.1. The material of the primary mirror with the 145 mm aperture is F-SILICA. Because of the high difficulty and cost in processing, the secondary mirror with 18 mm aperture is made of aluminum alloy[7].

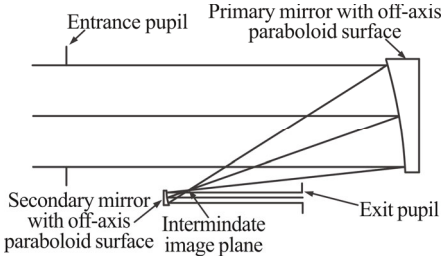

Fig.1 Optical system of the laser communication terminal

The laser communication terminal is mainly composed of the following components: the primary mirror component, the secondary mirror component and the main support frame, as shown in Fig.2. For the sake of meeting the requirement that the mass and the fundamental frequency of the terminal is less than 65 kg and more than 60 Hz, respectively, the titanium alloy is adopted to design the main support frame, which has high specific stiffness, low density and good thermal stability. The primary mirror component contains a primary mirror, a support and a backboard through which the primary mirror mounted on the support is connected with the main support. The support of the primary mirror is made of invar whose linear expansion efficient can be adjusted within the specified temperature range, achieving the match of thermal deformation with the primary mirror. In virtue of no-touch with the primary mirror, the backboard of the primary is made of titanium alloy. The secondary mirror component mainly contains a secondary mirror and a flexure support which is made of aluminum to achieve the match of thermal deformation with the secondary mirror. However, the material linear expansion coefficient difference between the secondary mirror component and the main support frame is so large that the sceondary mirror will produce great rigid body displacement and surface distortion under the condition of 20±2°C, which seriously affects the performance of the terminal. Therefore, the athermal design should be conducted to meet the high image quality requirement that the value of the wavefront aberration root mean square (*RMS*) is less than 1/20λ.

The flexure hinge, a common structure to reduce the effect on the mirror surface caused by the temperature and assembly stress through the local-elastic deformation, is widely adopted to design the mirror support, which possesses the superior characteristics as follows: low mass, high precision, frictionless, simple structure and high reliability. Traditionally, the design of the flexure hinge should be paid full attenation to its stiffness and flexibility at the same time[8], namely the stiffness of the flexure hinges is large enough to meet the index of the fundamental frequency, and the flexibility is large enough to reduce the effect on the mirror surface through the micro-elastic deformation under the condition of 20±2°C. In this paper, based on the design of the balance between the stiffness and flexibility, the layout and combination of the flexure hinges are studied to control the movement of the mirror caused by the temperature variation, and the integrated optimization model whose optimization objective and variable is the wavefront aberration of the terminal optical system and the structure parameters of the flexure hinges, respectively, is established to conduct the athermal design.

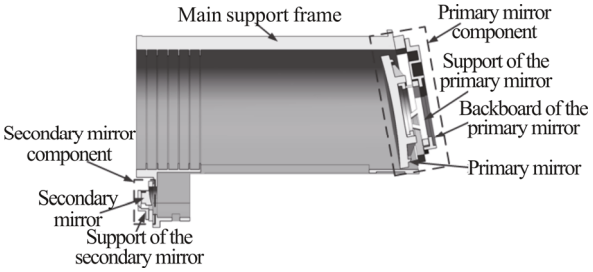

Fig.2 Ensemble scheme of the laser communication terminal

To satisfy the fundamental frequency index of the mirror support and reduce the effect of the support's deformation on the mirror surface as much as possible, the position of the flexure hinges is designed on the three outriggers and near the interface with the secondary mirror. Considering the complexity of the flexure hinges' processing method, the straight-circle flexure hinges is adopted to design the mirror support[9]. In order to increase the load path length and achieve the maximal variation range of the flexibility or stiffness with the limit of the flexure hinges' geometrical size, the layout of the flexure hinges is designed as follows: two straight-circle flexure hinges are series-wound on three outriggers, respectively, and the open direction is different, as shown in Fig.3. When the parameters of the flexure hinges on the three outriggers is set to be different, the deformation direction of the mirror support will change under the condition of 20±2°C.

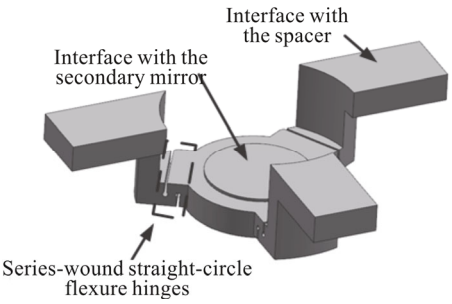

Fig.3 Secondary mirror support with flexure hinges

The math model is established to calculate the rotary flexibility or stiffness around the z-axis which is the main deformation form and key index of the flexure hinge, as shown in Fig.4. According to the mechanics theory of materials, the rotary flexibility can be expressed in formula as follows:

$$\frac{\theta}{M}=C_{o-z}=\frac{L}{EI}\ , \tag{1}$$

where θ is rotary angle of the flexure hinge, M is torque applied on the flexure hinge, $C_{o\text{-}z}$ is rotary flexibility of the flexure hinges around z-axis, L is length of the flexure hinge, E is elasticity modulus of the flexure hinge's material and I is inertia around the z-axis of the flexure hinge. Because the load path and contour of the flexure hinge is relatively complex, its rotary flexibility can not be estimated directly through Eq.(1). Through the method of the intergral theory and dividing the flexure hinges into three integral regions in Fig.4, the rotary flexibility can be expressed as follows[10]:

$$C_{O\text{-}Z}=\int_0^x\frac{\mathrm{d}x}{EI_z(x)}=\frac{12}{EW}\left\{\frac{H-2(r+t_1)}{t_2^{\,3}}+\right.$$
$$r(3\pi r(r+t_1)+2\sqrt{\frac{t_1(2r+t_1)}{(r+t_1)^2}}(3r^2+4rt_1+2t_1^{\,2})+$$
$$\left.6r(r+t_1)\arcsin[\frac{r}{r+t_1}])\right\}/$$
$$[(r+t)^5\left(\frac{t_1(2r+t_1)}{(r+t_1)^2}\right)^{5/2}]\ , \tag{2}$$

where r is radius of the inscribed cylinder, t_1 is minimum thickness, t_2 is separation distance between the two flexure hinges, W is width, and H is height.

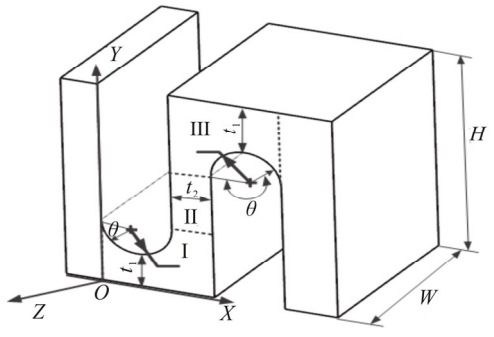

Fig.4 Stiffness analysis diagram of the series-wound right-circle flexure hinges

To reduce the complexity of the integrated optimization model as much as possible without affecting its accuracy, the sensitivity of the parameters are analyzed. With the constrains of the support geometrical size, the initial value and data range of the flexure hinge's parameters r, t_1 and t_2 are given in Tab.1. According to Eq.(2), the curve diagram of the relation between the flexibility and the parameters is plotted in Fig.5, which indicates that the parameters t_1 and t_2 are more sensitive than r for the flexibility of the flexure hinge. Therefore, taking into the consideration of the factors such as the calculation and the control efficiency, the parameter t_1 and t_2 are selected as the variable of the integrated optimization model.

Tab.1 Initial values and data ranges of the parameters r, t_1, t_2

Parameter	Initial value (mm)	Range (mm)
t_1	0.4	[0.1,4]
t_2	1.5	[0.1,4]
r	0.4	[0.1,2]

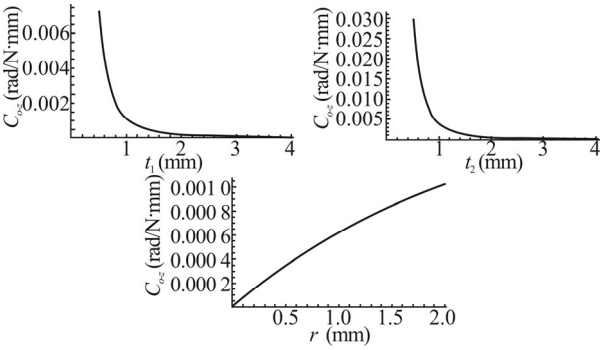

Fig.5 Relationship between the flexibility and the parameters of the flexure hinge

As demonstrated above, the relation between the parameters of the flexure hinges and its stiffness is one-to-one correspondence, which is the same as the relationship between the parameters and the coupling deformation caused by the mismatch of the linear expansion coefficient under the condition of 20±2℃. According to the theory of the optical system alignment, the relationship between the position of the mirror and the wavefront aberration value is a continuous function[11]. Therefore, according to the characteristic of the continuous function, the wavefront aberration value must have a maximum and a minimum value when the range of the flexure hinges parameters is a closed interval. So the integrated optimization model which consists of the mode calculation, the deformation calculation and the wavefront aberration calculation, is established as follow, to search a set parameters of the flexure hinges which minimizes the wavefront aberration value.

Minimize: $$W_{\text{error}}=F(S+\Delta S), \tag{3}$$

Subject to: $$f_1(t_1^i,t_2^i)\ge 60\ \text{Hz}$$
$$0\le t_1^i\le 4\ \text{mm};0\le t_2^i\le 4\ \text{mm}, \tag{4}$$

where $t_1{}^i$ and $t_2{}^i$ (i=1,2,3) is the parameters of the flexure hinges on the three outriggers, f_1 is the

fundamental frequency of the terminal, and the W_{error} is the wavefront aberration *RMS* value.

The flow based on the integrated optimization platform Isight is established to solve the integrated optimization model, as shown in Fig.6, which consists of data pre-processing, parameterization of the flexure hinges, calculation of the mode and the deformation, data conversion, wavefront aberration analysis and data analysis. The data pre-processing of the flow is employed to control the decimal place to satisfy the requirement of the processing method. The parameterization of the flexure hinges is employed to supply a interface between the variable of the integrated optimization model and the finite element model. The calculation of the mode and deformation is employed to supply the basic data for the calculation of the wavefront aberration. The data conversion is employed to transform the finite element node data of the mirror into the distortion and movement of the mirror, which is used for the calculation of the wavefront aberration *RMS* based on the software CODEV. In the integrated optimization flow, the finite element mode and the parameterization of the flexure hinges should be paid more attention to, which are the basis of the integrated optimization and seriously affect the calculation speed.

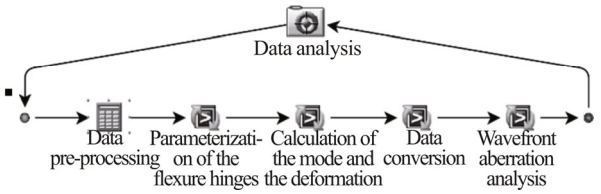

Fig.6 Flow of the integrated optimization

Finite element models are established to calculate the deformation of the mirror and the structure of the laser communication terminal under the condition of 20±2°C, as shown in Fig.7. Considering the computation speed and accuracy, the finite element models of the structure component are mainly composed of the hexahedral elements, and the rest is composed of the triangular prism elements and tetrahedron elements with ten nodes. The finite element model of the mirrors is composed of the combination of the shell elements and the hexahedral elements. The shell elements of the mirrors act as fitting of the mirror surface and the rigid displacement instead of the hexahedral elements, which greatly reduces the calculation of the mirror fitting and increases the calculation speed.

(a) Structure of the laser communication terminal

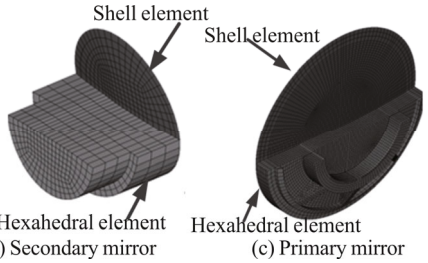

Fig.7 Finite element models of the structure, secondary mirror and the primary mirror

The parameterization of the flexure hinges is carried out based on the technology of the mesh morph, which can control the amount and direction of the element translation through the parameter. The domains are established to define the morphed region of the element and the position of the handles is the variable of the integrated optimization, as shown in Fig.8.

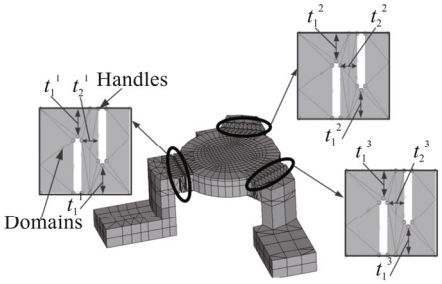

Fig.8 Parameterization of the secondary mirror flexure support finite element model

In view of the complexity of the optimization model, the amount of the variable, and the large calculation, the Multi-Island-Genetic algorithm, a global optimization algorithm with strong adaptability, is adopted to conduct the data analysis which determines the optimization tendency and the parameters to be used in next iteration. The optimization result indicates that the wavefront aberration is reduced by from 0.066λ to 0.042λ which is less than the 1/20λ, and the athermal design method is effective, as shown in Tab.2.

Tab.2 Optimization results of the flexure hinges' parameters and the wavefront aberration values

Variable	Initial value	Optimized value
t_1^1	0.4 mm	2.5 mm
t_1^2	0.4 mm	0.3 mm
t_1^3	0.4 mm	0.3 mm
t_2^1	2 mm	3.0 mm
t_2^2	2 mm	1.1 mm
t_2^3	2 mm	1.1 mm
w	0.066λ	0.042λ
f_1	320 Hz	318 Hz

In order to verify the athermal design validity of the mirror flexure support of the laser communication terminal, the components such as the main support frame,

the primary mirror component and the secondary mirror component are designed based on the simulation result above and manufactured. The prototype is constructed as shown in Fig.9, which consists of the laser communication terminal, the interferometer acting as measuring the wavefront aberration and the theodolite acting as adjustment. Some experimental tests are conducted under the condition of 20±2°C. The positions of the temperature data collection are shown in Fig.10.

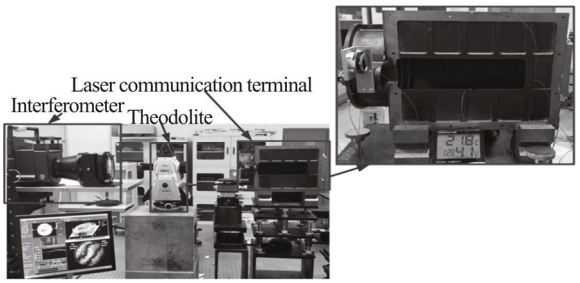

Fig.9 Experimental prototype

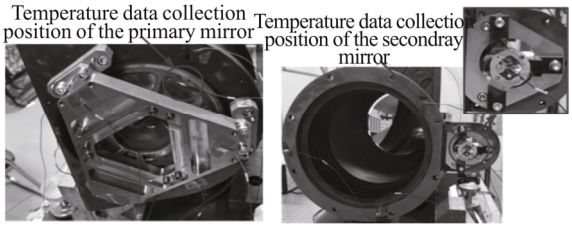

Fig.10 Positions of the temperature data collection

The experimental results indicate that the maximum of the wavefront aberration *RMS* is 0.043λ under the condition of 20±2°C, which satisfies the index of the laser communication terminal, as shown in Tab.3, and the error between the simulation result and the experimental result is less than 10%, which shows the athermal design is correct.

Tab.3 Wavefront aberration *RMS* under different temperatures

Primary mirror's temperature	Secondary mirror's temperature	Wavefront aberration *RMS*		
		Original test results	Optimized test results	Simulation results
18.21°C	18.22°C	0.062λ	0.041λ	0.039λ
19.03°C	19.11°C	0.048λ	0.033λ	0.03λ
20.05°C	20.07°C	0.032λ	0.032λ	0.029λ
21.10°C	21.19°C	0.053λ	0.034λ	0.03λ
21.91°C	22.20°C	0.066λ	0.043λ	0.041λ

In conclusion, the athermal design of the mirror support with the flexure hinges for the laser communication terminal has been studied in detail. Based on layout of the flexure hinges, the integrated optimization model whose objective is the value of the wavefront aberration *RMS* has been established and the parameters of the flexure hinges, which are variables of the model, have been determined through the technology of the integrated optimization. The prototype of the terminal has been constructed and some experimental have been carried out. Experimental results indicate that the wavefront aberration *RMS* is less than 1/20λ, which can meet the requirement of the laser communication terminal, providing some referenced value for the small aperture mirror support in the off-axis optical system.

References

[1] NI Ying-xue, WU Jia-bin, SAN Xiao-gang, Gao Shi-jie, DING Shao-hang, WANG Jing, WANG Tao and WANG Hui-xian, Optoelectronics Letters **14**, 48 (2018).

[2] Gao Duo-rui, Li Tian-lun and Sun Yue, Chinese Optics **6**, 901 (2018).

[3] WU Qian-qian, ZHANG Xin-ting, LIANG Jing, LIU Yun and LI Xiao-qi, Meteorological, Hydrological and Marine Instruments **4**, 59 (2017).

[4] Li Shen-hua, Guan Ying-jun and Xin Hong-wei, Laser & infrared **11**, 1422 (2017). (in Chinese)

[5] Liu Ming, Zhang Li-zong and Li Xiang, Opto-Electronic Engineering **5**, 47 (2018).

[6] Ren Guo-rui, Li Chuang and Pang Zhi-hai, Design and Test of a Flexure Mount for Lightweight Mirror, Proc. SPIE, 10837 (2018).

[7] Tan Shuang-long, Wang Ling-jie and Zhang Xin, Journal of Changchun University of Science and Technology **40**, 5 (2017).

[8] Zhang Wei, Yang Li-bao and Li Qing-ya, Infrared and Laser Engineering **11**, 258 (2018). (in Chinese)

[9] Li Yao, Wu Hong-tao and Yang Xiao-long, Optics and Precision Engineering **6**, 1370 (2018). (in Chinese)

[10] Qiu Li-fang, Chen Hai-xiang and Wu You-wei, Journal of Beijing University of Aeronautics and Astronautics **6**, 1133 (2018). (in Chinese)

[11] Ju Guo-hao, Research on Active Optical Wavefront Control Methods for Off-axis Reflective Astronomical Telescopes, Beijing: University of Chinese Academy of Sciences, 2017. (in Chinese)